OTKA NF 84006

Final Report

Behind Host-Microbe Interactions: Functional and structural analysis of virulence factors of *Candida parapsilosis*.

Gazda-Patogén kölcsönhatások nyomában: *Candida parapsilosis* virulencia faktorainak strukturális és funkcionális vizsgálata.

Attila Gacser PhD
University of Szeged
Department of Microbiology

30.09.2015.

Summary

Candida albicans (Ca) and Candida parapsilosis (Cp) are the two main yeast species that are both commensal of humans and responsible for devastating disseminated infections. The aim of this NF84006 project was to investigate the virulence and the pathomechanisms of the important human fungal pathogen *Candida parapsilosis*. First we established and further developed in vitro and in vivo infection models to examine host pathogen interactions. We adapted in vitro models using cell lines (J774.2 murine macrophages, THP-1 human macrophages) or primary cells (Bone marrow derived macrophages from mouse, peripherial mononuclear cell derived macrophages from human). We showed that fungal lipases can reduce host inflammatory response and proved their role in the pathogenesis. We investigated the cellular immune response orchestred by phagocytes. We proved the crucial role of defensins in the host anti-Candida response and we were the first to show the major differences in the T cell response upon *Candida parapsilosis* infections in comparison to *Candida albicans in vitro*.
Majority of our results were already published (see detailed publication list attached to the final report), below we report about the unpublished data. Importantly, the preparation of two manuscripts describing some of the below discussed data is also in progress. Estimated publishing time is in 2016.

The detailed Report about the unpublished results:

1. Composition of fungal cell wall as the first line of host recognition:
Since the last few decades number of fungal diseases has been increased. The leading causes of these infections are *Candida* species. However, these species are part of the healthy human microbiome; they are also capable to switch pathogenic. Pathogenic switch usually occur in patient with immunocompromised state, organ transplantation or premature neonates according to wide range of surveillance data. Although, *C. albicans* is the most frequent causative agent of candidiasis, importance of other *Candida* species such as *C. glabrata*, *C. parapsilosis* and *C. tropicalis* have increased in the near past. *C. albicans* and *C. parapsilosis* show differences not just in the epidemiology, but also in the immune response and recognition of the two species. *C. parapsilosis* cause infections more frequently in neonates then the *C. albicans*. At some geographic regions *C. parapsilosis* cause more infections than any other *Candida* species in every age group.
C. parapsilosis is only producing pseudo hyphae instead of true hyphae like *C. albicans*. Several studies have shown pseudo hyphae growing cells has the same cell wall composition as the yeast growing cells, however true hyphae has a completely altered cell wall structure. Fungal cell wall contains three major component of the cell wall. These are chitin, β-D glucan and mannose from the plasma membrane to outside of the wall, respectively (Fig. 1.). *C. albicans* cell wall structure and its role in infection is a well-studied field of fungal pathogenesis, however, less known about *C. parapsilosis*. To investigate important genetic factors in the cell

wall structure we have examined the cell wall composition of different strains containing deletion for different transcription factors.

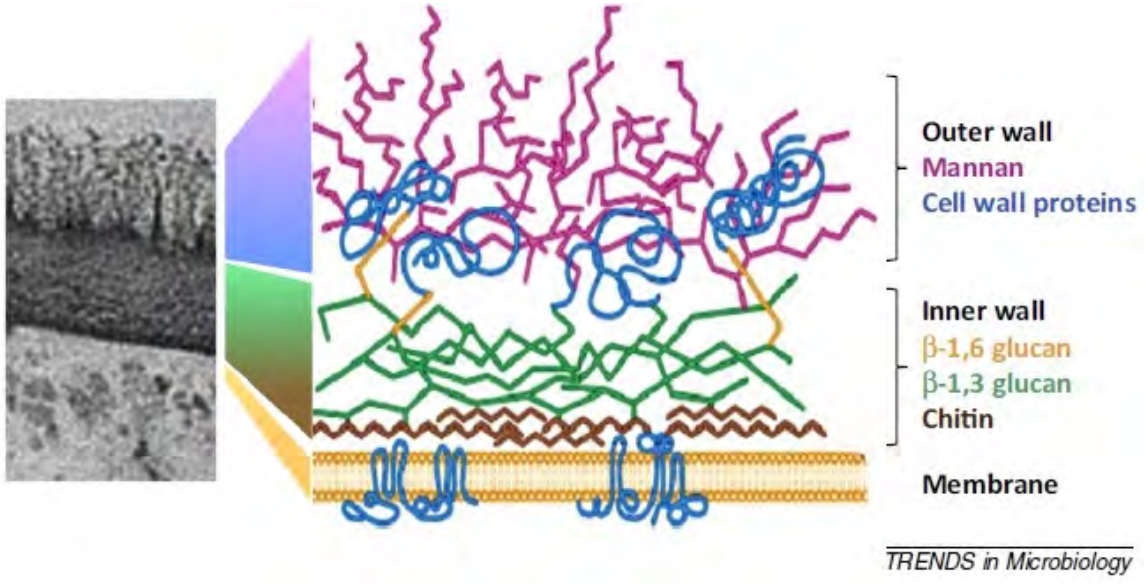

Fig. 1.: Structure of fungal cell wall
(Alistair J.P. Brown et. al., *Trends in Microb.* 2014; 22(11): 614-622)

Investigation of particular mutants from Knock out Library

We previously generated a unique gene knock out library in *Candida parapsilosis* using the fusion PCR method. Specific genes were chosen for knock out according to RNA-seq data from THP-1 infection experiment (see later in the report). In the frame of this project there have already been produced 29 knock out strains independently twice in parallel. During phenotypic characterization of these strains four of them were chosen for further analysis according to their changed phenotype in the presence of cell wall stressors such as calcofluor white, congo red and caffeine. Investigated strains were:

C. p. Δ/Δ CPAR2_100540 13/1
C. p. Δ/Δ CPAR2_100540 13/2
C. p. Δ/Δ CPAR2_200390 1/1
C. p. Δ/Δ CPAR2_200390 2/2
C. p. Δ/Δ CPAR2_303700 4/2
C. p. Δ/Δ CPAR2_303700 4/3
C. p. Δ/Δ CPAR2_602840 1/1

Different cell wall components of the defined strains were investigated on the behalf of alterations in the cell wall. Multiple dyes are available to stain the particular components of fungal cell wall. The main components of the fungal cell wall are chitin, β-1,3-glucane, β-1,6-glucane and α-mannans, on certain parts of the fungal surfaces chitin-oligomers are also present (most of it at “budscars”). The appropriate dyes for these cell wall components are Calcofluor White, Aniline Blue, ConcanavalinA-FITC (ConA-FITC) and Wheat Germ Agglutinin-

TRITC (WGA-TRITC), respectively. Two KO mutants from the four investigated strains showed altered cell wall composition using confocal microscopy.

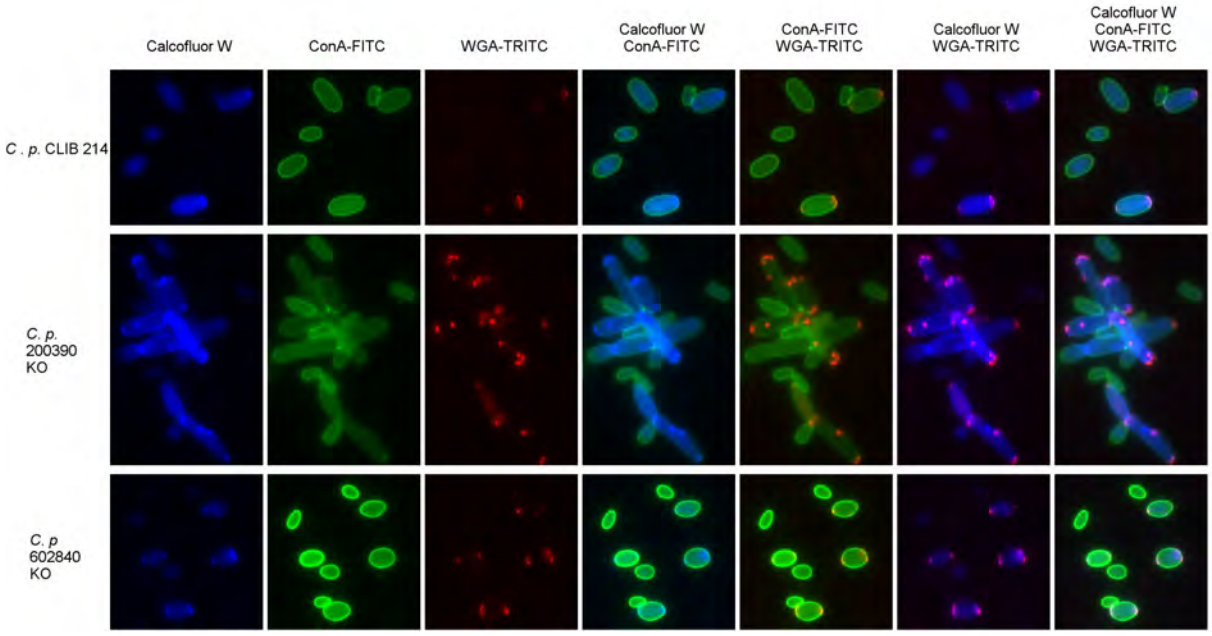

Fig. 2.: Calcofluor White, ConA-FITC and WGA-TRITC staining of strains: *C. p.*CLIB 214 WT, *C. p.* Δ/Δ CPAR2_200390 and *C. p.* Δ/Δ CPAR2_602840

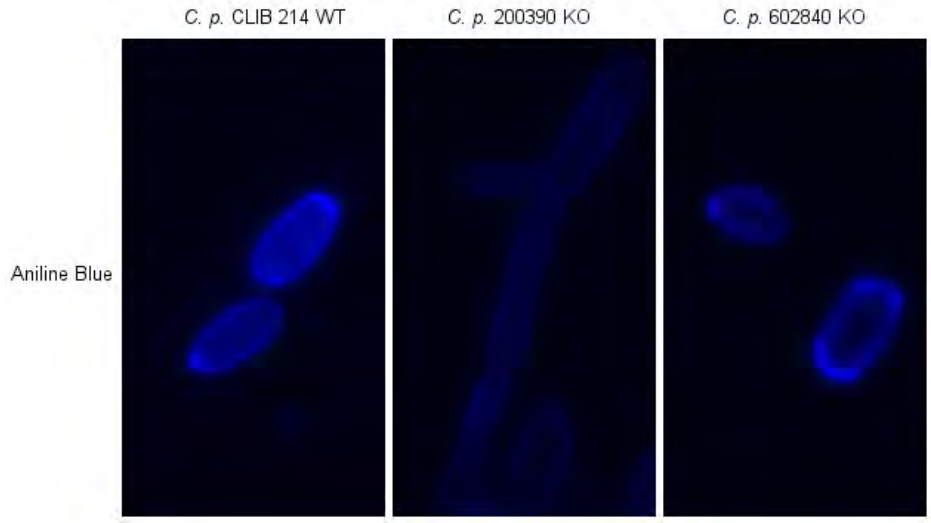

Fig. 3.: Aniline Blue staining of strains: *C. p.* CLIB 214 WT, *C. p.* Δ/Δ CPAR2_200390 and *C. p.* Δ/Δ CPAR2_602840

C. p. Δ/Δ CPAR2_602840 strain showed slight decrease in β-glucan content (Fig. 3.), but staining with ConA-FITC was stronger in compare to the *C. p.* CLIB 214 WT revealing the increased mannan content of the cell wall of this strain (Fig. 2.).

β-glucan in the cell wall of *C. p.* Δ/Δ CPAR2_200390 were decreased significantly compared to the wild type (Fig. 2.). This strain was able to produce pseudo hyphae in a large amount. The elongated pseudo hyphae forming cells have had more chitin in the cell wall; however, normal yeast cells have the same amount of chitin as the wild type, which is only growing in yeast

form. Interestingly pseudo hyphae forming cells also exposed more chitin-oligomers then wild type cells and not only at the tip of elongated cells, but also on the surface of lateral parts (Fig. 2. and Fig. 4.).

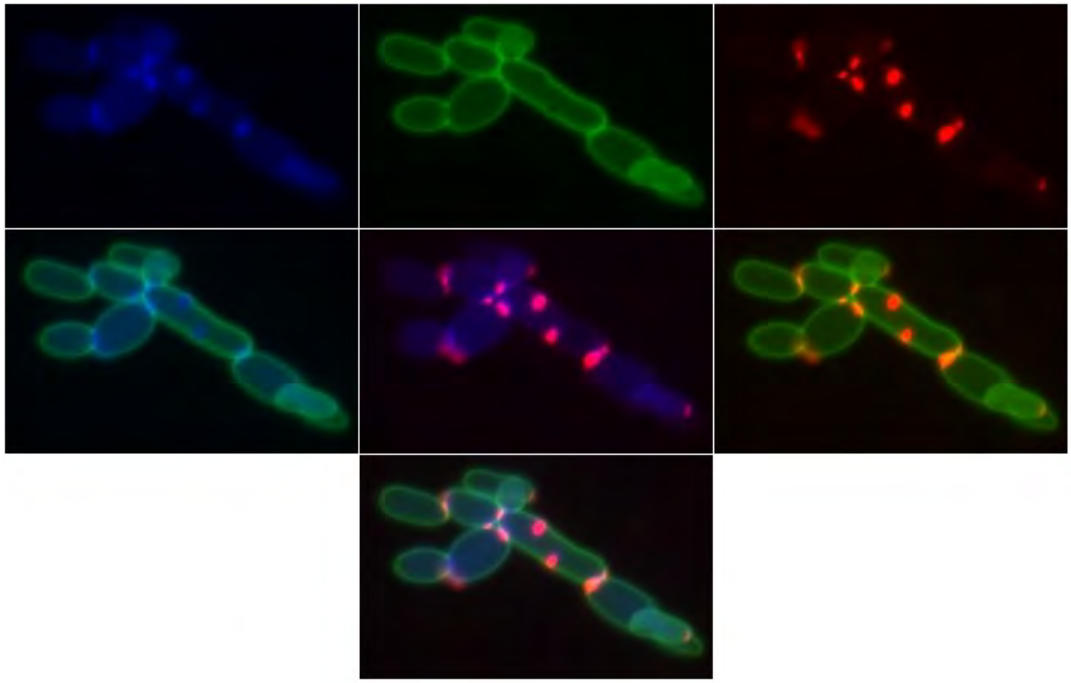

Fig. 4.: Calcofluor White, ConA-FITC and WGA-TRITC staining of *C. p.* Δ/Δ CPAR2_200390

Scanning electron microscopy images of the four different KO mutants were also performed. Figure 6. shows the scanning electrographic image of the *C. p.* Δ/Δ CPAR2_200390 strain. Interestingly, there were no recognizable bud scars at the lateral part of the elongated pseudo hyphae cells; bud scars were detectable only at the tip of the pseudo hyphae (Fig. 6. red arrow). This finding suggests, that digested or exposed chitin is presented more often at the surface of the mutant producing pseudo hyphae, compared to the wild type. Normally in *C. parapsilosis* new daughter cells start to grow only after the other daughter cell separated from the mother cell (Fig. 5. A). However, by the mutant *C. p.* Δ/Δ CPAR2_200390 showed interesting phenotype during pseudo hyphae production, since the new daughter cells start to grow before separation of older daughter cell (Fig. 5. B).

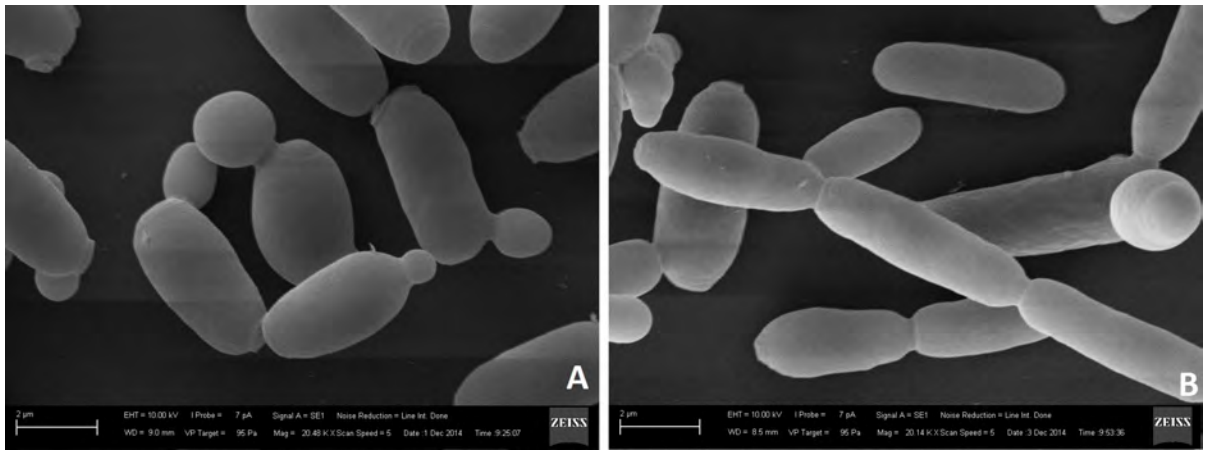

Fig. 5.: SEM image of (A) wild type and (B) *C. p.* Δ/Δ CPAR2_200390

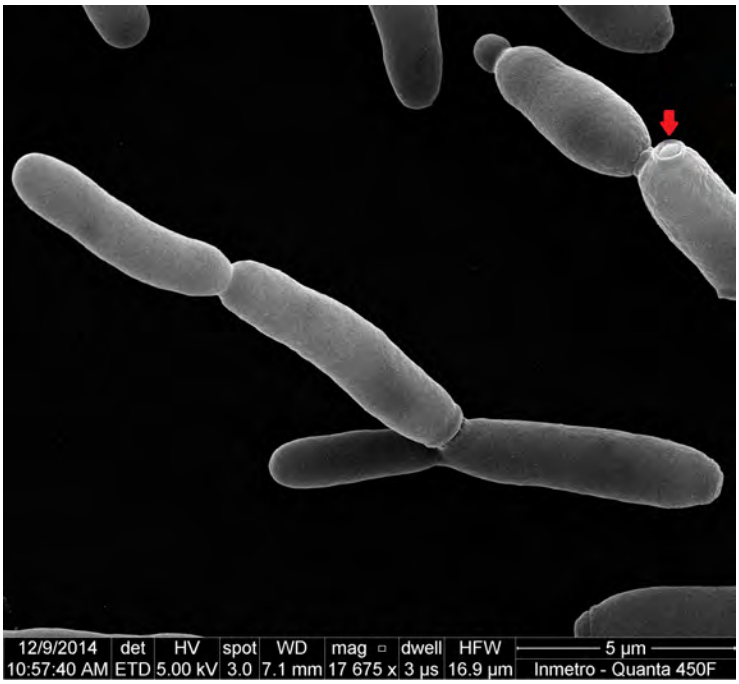

Fig. 6.: SEM image of *C. p.* Δ/Δ CPAR2_200390 Red arrow: bud scar

Investigation of *C. parapsilosis OCH1* KO and overexpression strains

A mannose compound of the cell wall is attached to other cell wall component via cell wall proteins (CWP) with N- or O-covalent bound. *OCH1* is a fungal gene coding α-1,6-mannosyltransferase, which is responsible for synthesis of large mannose side chains on O-linked mannane (Fig. 7.).

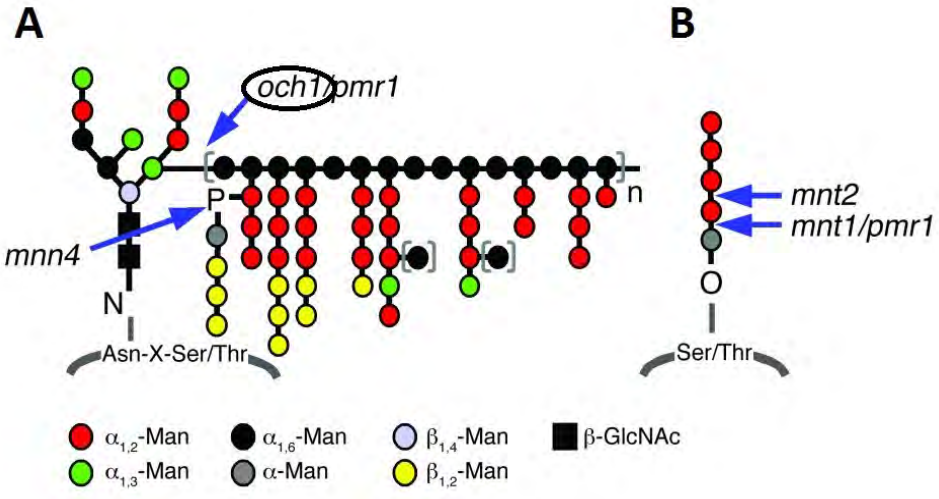

Fig. 7.: Schematic image of cell wall protein (CWP) N- (A) and O-linked (B) mannosilation (Mihai G. Netea et. al., *J Clin Invest.* 2006;116(6):1642-1650)

We previously generated both *OCH1* gene deletion and overexpression derivative from Candida parapsilosis GA1 strain. *OCH1* KO strain had an altered cell wall structure compared to

the wild type and to the *OCH1* overexpressing mutants. Chitin and the chitin-oligomers were present in a higher level in the cell wall of KO strain (Fig. 8.). Oligomerized chitin was present in an increased level only at the bud scars. Mannose content in the cell wall of KO mutant was accumulated in the area close to the bud scars.

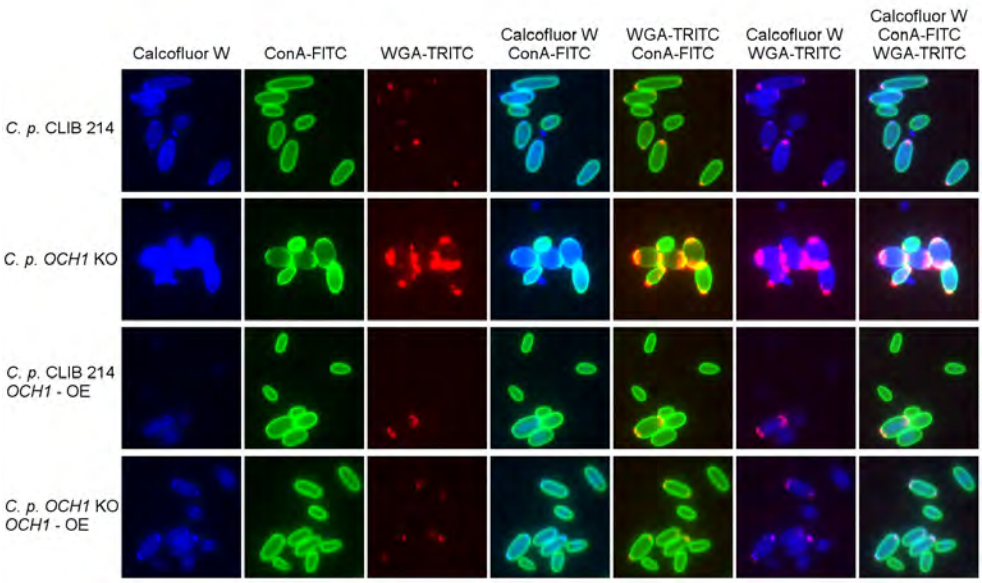

Fig. 8.: Cell wall staining of *OCH1* related strains Blue: chitin, Green: mannose, Red: chitin-oligomers

For further investigation of cell wall structure of *OCH1* related strains, samples of strains were subjected for TEM analysis. TEM images have been already taken from *C. p.* GA1 and *C. p.* Δ/Δ *och1* strains. The outer, most electron dense part of the cell wall was thinner in the case of the *C. p.* Δ/Δ *och1* (Fig. 9. B,) strain compared to the cell wall of wild type strain (Fig. 9. A,). This part of fungal cell wall contains mannose and manno-proteins, thus our result suggest a strong alteration in the most outer layer of the *OCH1* mutant.

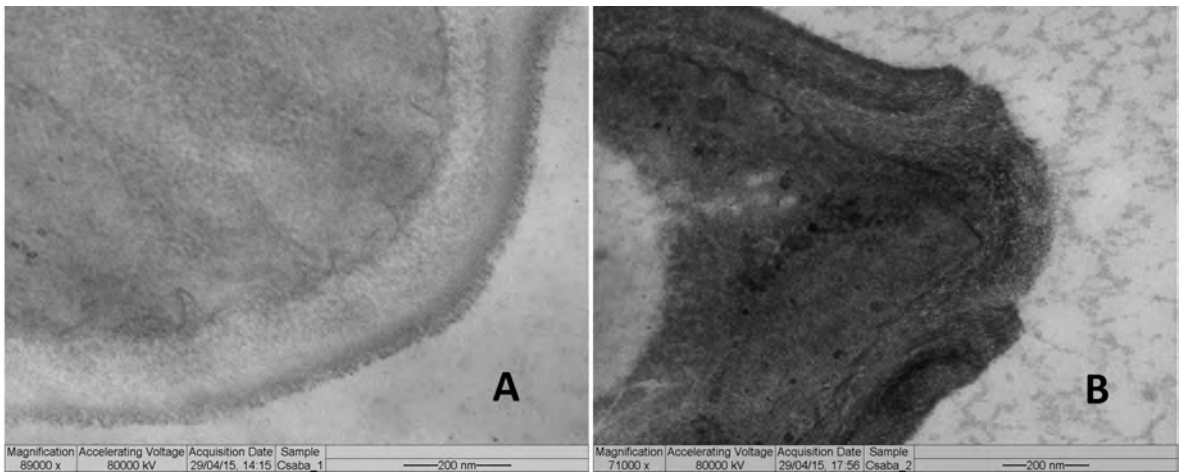

Fig.9.: Transmission electromicrographic images of A, *C. p.* GA1 and B, *C. p.* Δ/Δ *och1* strains

In summary we identified some promissing cell wall mutants, that can help us to disect the host-pathogen interactions in more depth. We expect to publish our data in the near future.

2. Development of an *in vitro* model system to study the interaction between murine macrophages and *C. parapsilosis*

The response of J774.2 murine macrophages given to *C. parapsilosis* clinical isolate was observed by flow cytometer, scanning electron microscope (**Fig. 10.**), flourescent microscope and confocal fluorescent microscope. It was established that J774.2 macrophages start to uptake *C. parapsilosis* wild-type cells after 30 minutes of incubation.

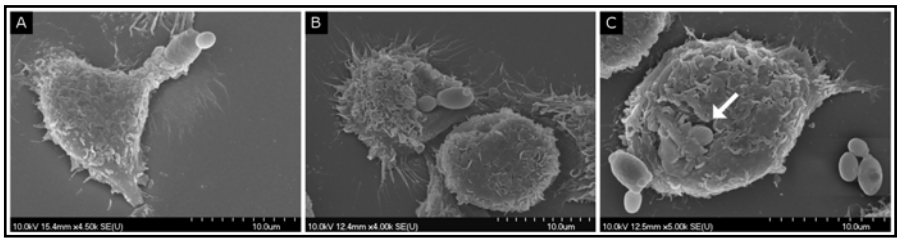

Fig. 10. Scanning electron microscopic images of stages of *C. parapsilosis* uptake by J774.2 murine macrophages.

The uptake reached a plateau-phase by the third hour. Phagosome-lysosome colocalisation and elimination of the yeasts occured by the eighth hour (**Fig. 11**).

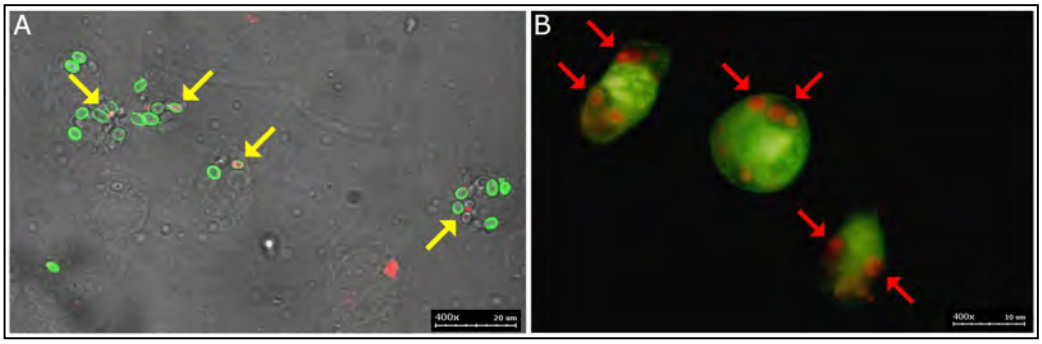

Fig. 11. Fluorescent microscopic pictures of J774.2 - C. parapsilosis interaction after 8 hours of co-incubation. Yellow arrows indicate strong colocalisation between internalised yeast cells and phagosomes (FITC/Lysotracker red staining) (A). Red arrows show dead fungi inside the phagosome (Acridin orange/Crystal violet staining) (B).

Since three and eight hours seemed to be important milestones of the interaction microarray analysis of the host transcriptome was performed with RNA samples isolated at these timepoints from the host. Respectively 115 and 511 genes were found to be differently expressed compared to the non-infected control. Genes taking part mostly in wound healing, stress or immune response were upregulated. The expression levels of genes (*CD83*, *IL1β*, *IL15*, *TNFα, TNFRSF9* and *PTGS-2*) choosen to validate these data by qRT-PCR supported the results of the microarray experiment (**Fig. 12.**).

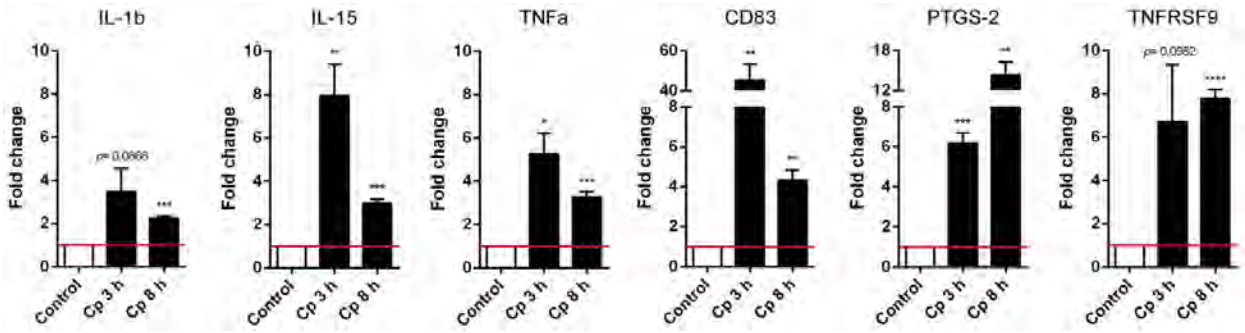

Fig. 12. Validation of RNA microarray data by qRT-PCR. Relative overexpression of selected genes of J774.2 macrophages were determined after 3 and 8 hours of co-incubation with *C. parapsilosis*.

The overexpression of the *TNFRSF9* gene was examined after stimulation by other *Candida* spp (*C. albicans*, *C. glabrata*, *C. guilliermondii*, *C. krusei*, *C. metapsilosis*, *C. orthopsilosis*, *C. tropicalis*) and both of them were able to induce the upregulation of *TNFRSF9*.
Flow cytometry analysis established that *C. parapsilosis* GA1 wild-type was able to increase the level of the functional protein on the surface of the phagocytes compared to the control (0 h).
The expression of this specific molecule was also examined *in vitro* in a model using mouse peritoneal macrophages and human PMBC derived macrophages after 3, 6, 12 and 24 hours of coincubation with wild-type *C. parapsilosis* GA1 strain. Both induced the overexpression of *TNFRSF9* in these cells. In mouse macrophages the longer the incubation time was, the higher the expression occured. In primary human cells however the highest expression was observed at twelve hours post-infection.

3. Whole transcriptome analysis of *C. parapsilosis sensu lato* group from *in vitro* interaction with THP-1 human monocytic cells

Complete transcriptional profile of the whole *C. parapsilosis sensu lato* group was characterised upon interaction with phagocytes. Yeast cells were stimulated with THP-1 human monocytes and RNA samples isolated after different periods of time were analysed by RNA-seq. One *C. metapsilosis*, one *C. orthopsilosis* and four *C. parapsilosis* strains were involved and a total of four timepoints (1h, 3, 6, 12h) were choosen for better resolution. *In silico* analysis determined the upregulated genes during infection (**Fig. 13.**).

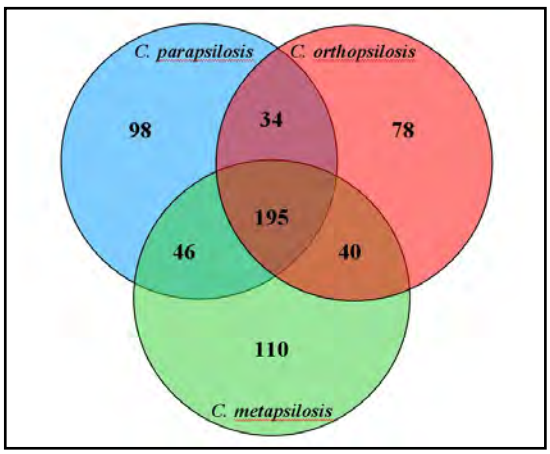

Fig. 13. Number and distribution of differentially expressed genes of the *C. parapsilosis sensu lato* species after 1 hour of co-incubation with THP-1 monocytes.

The interaction of THP-1 with two environmental (CBS 1954 and CBS 6318) and two clinical (CDC317 and GA1) strains was also examined. Based on the heatmap of the Euclidean-distances of the samples from this arrangement the clinical and environmental *C. parapsilos*is isolates were classified in completely different clusters suggesting notable differences in the transciptomes. In the four strains a total of 5.167 transcripts were identified. Out of these 729 transcripts were found to be differentially expressed in the presence of monocytes at the first hour of the stimulation.
The thirty genes with the highest expression difference were choosen at any given timepoints to calculate the Euclidean-distances of the samples. This analysis included the following four layout: 1.) basic expression (without monocytes) of the two clinical versus the two environmental isolates, 2.) the two environmental strains uninduced versus induced at 1h, and 3.)/4.) the two clinical isolates uninduced versus induced at 3 h and 12 h. Each two groups of the four comparison aligned into separate clusters, referring differences in the expressions between the examined groups.
Being the clinically most relevant species of the *sensu lato* group, the transcriptional profile of *C. parapsilosis* was analysed more in detail so far. Among genes overexpressed in this species in the presence of human monocytes, 75 kinases and transcriptional factors were identified. This set of genes can be considered as potential regulators of virulence factors. To prove this hypothesis and characterise the role of these genes more in detail a knock-out and overexpression library as well as an inducable gene expression system is being created involving these candidates.

4. Comparative genomic analysis of the *Candida parapsilosis sensu lato* group

Since the members of the *C. parapsilosis sensu lato* are closely related and at the same time they possess different virulence attributes, they offer a unique opportunity to characterise genome evolution and virulence factors for adoptation to the human environment. Comparative genomic analysis makes possible to get insights into the genome plasticity and therefore the evolution of these species.

Candida parapsilosis

Our earlier results revealed notable differences between clinical and environmental isolates of *C. parapsilosis* regarding their resistance to phagocytosis and monocyte elimination mechanisms, the distribution of the members of the *ALS* (Agglutinin-like sequences)

genefamily, and chromosome arrangements. To map the genomic variation of *C. parapsilosis* isolates originated from different sources whole genom sequencing was carried out involving two environmental (CBS 1954 and CBS 6318) and GA1 clinical isolates, then comparative genomic analysis was performed including CDC317 strain as a reference.
In silico analysis identified a total of 5.147 SNPs and determined the distribution of these in CBS 1954, CBS 6318 and GA1 compared to the CDC317. Although evidence of recombination has never been described in this species, the frequency and distribution of these SNPs refers to this molecular event.
The comparison predicted forty chromosomal mutations: five duplications (DUP) and 35 deletions (DEL). The 35 deletions range from 17 to 23.475 bps. Out of these 31 affected protein coding regions and 18 seem to led gene fusions. Most of them are specific to one single strain. Five deletions were found to be heterozygous. Twenty out of the 35 deletions were choosen for experimental validation. PCR and Southern hybridisation strategies were designed and applied together with Sanger sequencing. The analysis of the flanking sites of specific deletions revealed nucleotide patterns referring to recombination events and Single Strand Annealing (SSA) as a mechanism for double strand break repair. Results of molecular techniques verified the *in silico* findings in 19 cases out of 20 the deletions choosen for experimental validation. Out of the five predicted heterozygous region three were confirmed. A deletion specific only for environmental strains was identified, that was not predictided by *in silico* data. The DUP#5 causes the copy number variation of a physiologically important gene named *ARR3*, that is an ortholog of the *S. cerevisiae ARR3* (arsenite transporter). This was found to be responsible for arsenite resistance in baker's yeast. The copy number variation and the flanking sequences of the copies of this gene in clinical isolates supports the idea that the "environment to host" transition occured more than once during the phylogeny of this species. This recognition contradict the present point of view that considers all clinical *C. parapsilosis* isolates being clonal.

Candida orthopsilosis

Based on differences in the ITS and MAT loci *Candida orthopsilosis* isolates can be placed into two subspecies called Type 1 and Type 2. Since there was only Type 2 (90-125) whole genome available, MCO456 (isolated from bloodstream infection in Texas, USA, previously classified as Type 1 by PCR) was choosen for genome sequencing and comparison. *In silico* analysis identified 103 deletions and 29 duplications out of which 17 were found to be shared by the two strains. Expansion of gene families related to virulence (efflux-pumps, lipases, secreted proteases, genes involved in antibiotic resistance) could have been observed. Nearly half (40) of the deletions were flanked by DNA direct repeats suggesting similar repair mechanism as the one of *C. parapsilosis*. Interestingly in contrast to 90-125, MCO456 seemed to be highly heterozygous. The average divergence in the heterozygous fragments was 4.5% and these heterozygous regions represented 17% of the whole genome. Moreover, 41% of MCO456 genome was found nearly identical to the one of 90-125 suggesting that the MCO456 identified

as Type 2, is actually a hybrid of two parental lineages, possibly come into existance via meiosis, one of which being very close relative of a Type 2 strain. This is supported by the finding that mitochondrial genomes of the two strains are almost identical. Regions of ITS and MAT locus though could have acquired from a Type 1 ancestor. Comparative genomic was carried out involving the genome of MCO456 and the partial genome available of AY2 (isolated from skin infection in Singapore) and a 99.997% percent identitiy was established at DNA level. Although the sampling is limited to 3 species, still these findings taken together might refer hybridisation a way to improve virulence attributes by combining genomes and increase survival odds in the host environment. Though it is not clear if it occurs in the nature or it is triggered by the human host, anyway the high similarity between strains from geographically distant locations suggests that these share common ancestors and spreaded globally.

Candida metapsilosis

A total of 11 *C. metapsilosis* clinical isolates from very distant geographical regions were choosen for genome sequencing and further analysis. Both strains were identified as diploids but contrary to *C. orthopsilosis* none of them was found to be homozygous. The average divergence of alleles in heterozygous regions was as high as in the case of *C. orthopsilosis* (4.5%). However fractions of heterozygous regions relative to the total length of the genome was extremely high, it varied among isolates and ranged from 54.5% to 61.3%. Distribution of LOH (Loss of heterozygosity) blocks among strains referring to one single hybridisation event in the past resulting in a hybrid spreaded worldwide without human mediation similar to *C. parpapsilosis*. This hypothesis is also supported by CNV (Copy number variation) data as 31 deletions (out of 82) and 15 duplications (out of 86) were shared by all strains. Although *C. parapsilosis sensu lato* species are known as fungi uncapable of meiosis, the presence of MTLα and MTLa idiomporphs in 10 out of the 11 sequenced isolates suggests that mating could have been the way of hybrid formation.

5. Comparative genomics of *Candida parapsilosis sensu lato* species complex

Since the genomic sequences of the *sensu lato* species were available, a whole genome comparison could have been performed for the first time. Phylogenetic reconstructions regarding synteny, single-copy orthologs and mitochondrial genomes resulted in a largely congruent phylogeny supporting a basal position to *C. metapsilosis*. 5,045 orthologous groups were found to be present in all species out of the total 5,743 orthologous groups identified. 4,574 were as one-to-one orthologs, meanwhile 226, 107 and 124 groups contained *C. metapsilosis*, *C. orthopsilosis* and *C. parapsilosis* specific paralogs, respectively. *In silico* analysis was carried out to discover the distribution of virulence related genes among the three species. It was established that *C. parapsilosis* and *C. metapsilosis* possess equal number of genes encoding secreted lipases (5), secreted proteases (14) and proteins with extracellular CFEM domains responsible for iron acquisition (7), outranking *C. orthopsilosis* that encodes 4,

11, 5 of these genes respectively. These findings though do not correlate with experimental results, as *C. metapsilosis* was found to be a species unable to produce secreted lipases (under experimental circumstances) possibly due to these genes in *C. metapsilosis* might be pseudogenes, or strongly repressed. The *ALS* genes, that responsible for adhesion in *C. albicans*, showed unequal distribution in the *C. parapsilosis* sensu lato complex. There were 5 *ALS* genes found in *C. parapsilosis*, *C. orthopsilosis* and *C. metapsilosis* encode only one but not the same, since the one in *C. metapsilosis* is close to CPAR2_404790, meanwhile the one of *C. orthopsilosis* encodes an ortholog closer to CPAR2_404800. Possessing more adhesins might open a gate for better adoptation to the environment and maybe to the human host as well. *In silico* analysis revealed obvious correlation between virulence attributes and expansion of gene families related to virulence only in the case of *ALS* genes. However especially the case of *C. metapsiolsis* secreted lipases underline the necessitiy of validation of computational analyses.

6. A murine neonate model for *C. parapsilosis* systemic infection

C. parapsilosis is the second or third most frequently identified pathogen in invasive candidiasis; besides, incidence of this opportunistic fungal pathogen is particularly high in premature infants, and it is often associated with neonatal mortality. A reliable animal model for disseminated candidiasis in the neonate is needed to study the unique aspects of this host-pathogen interaction. We created a murine model of disseminated *candidiasis* in neonates using two days old BALB/C pups. In this model, we inoculated the mouse pups via retro-orbital intravenous injections with inocula of *C.parapsilosis* strains.

We have previously shown that *N*-linked mannosyl residues play an important role in the virulence of *C. parapsilosis* in *in vivo* mouse model. Neonatal mouse model have been successfully used to study the role of this cell wall component: we found that neonate mice infected with the *och1Δ C. parapsilosis* had significantly decreased fungal burdens in the spleen, kidneys and liver at 2 or 7 days post-infection. In this study we found significant differences in the susceptibility of mice, that can be defined between the neonatal and adult host and demonstrate the importance of neonatal models to study invasive disease (Fig. 20).

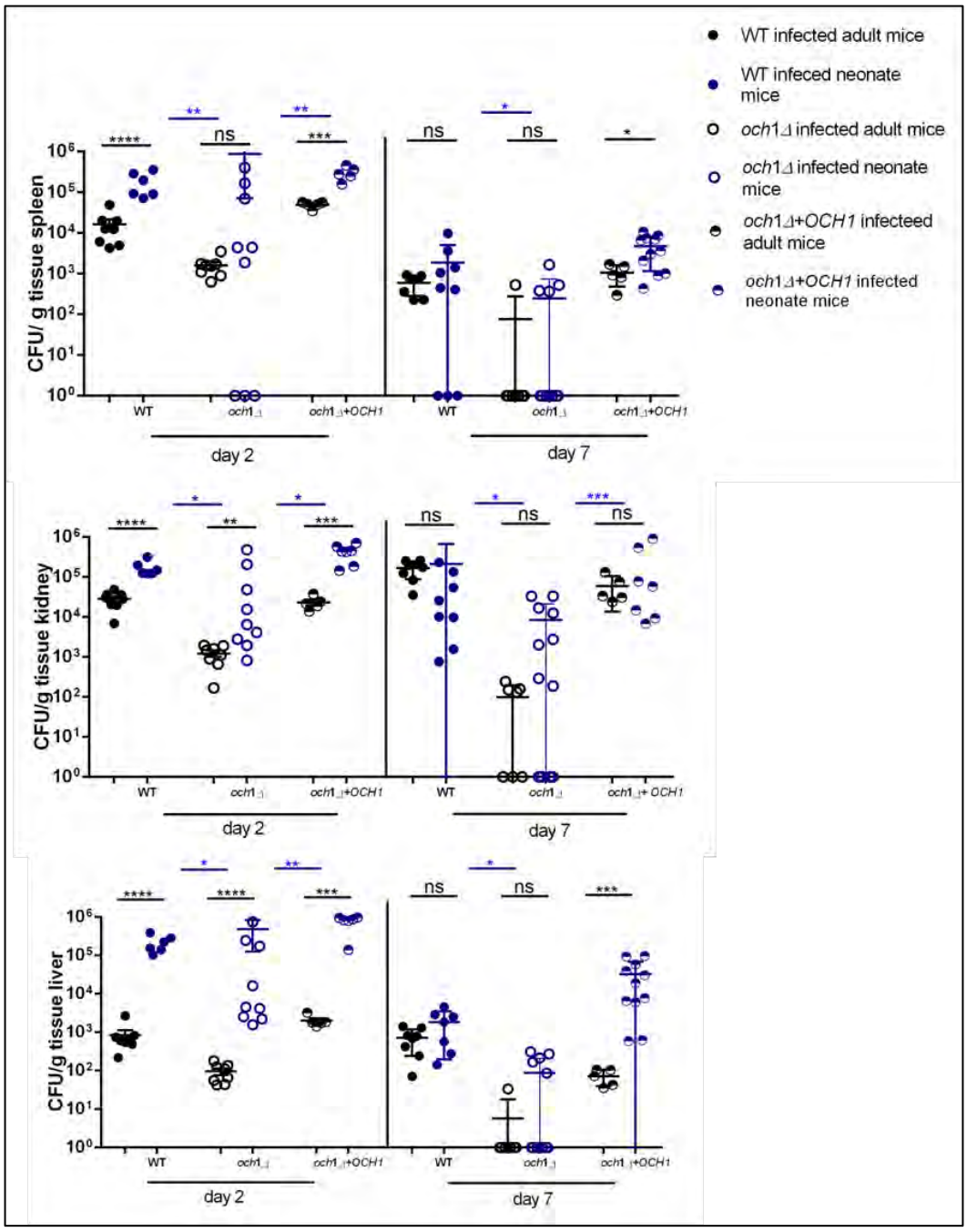

Fig. 14. Timed pregnant BALB/c mice were monitored to determine the date of parturition. Pups were delivered in litters ranging from 3-9 pups and were randomized prior to inoculation of *C. parapsilosis* yeast. Pups were injected on post-partum day 2. Just prior to injection, each pup was weighed to the nearest tenth of a gram. Weight of pups was closely clustered around 2 g, so each pup received a standard dose of 20 µl 2x 10^7 colony forming units or sterile PBS (control) injected retro-orbital i.v. infection. After 1, 2 or 7 days post infection, animals were euthanized, and liver, kidneys and spleen were aseptically removed, weighed, and homogenized in sterile PBS using a tissue grinder. The fungal burdens in these tissues were determined by plating serial dilutions onto three YPD agar plates per tissue. The CFUs were counted after 48 h of incubation at 30°C and expressed as CFU/g tissue. Data are presented as

means +/- SEM. Results are pooled data from 2 separate experiments with a total of 8 mice per group. *p<0.05, ** p<0.01, *** p<0.001, **** p<0.0001

7. Comparison of immune responses in human PBMCs following stimulation with *C. parapsilosis* and *C. albicans*

Comparison of T-cell polarization induced by C. parapsilosis and C. albicans

First, we compared the pro-inflammatory cytokine production in PBMCs following stimulation with heat-killed *C. parapsilosis* and *C. albicans*. We found that PBMCs stimulated with *C. parapsilosis* produced similar quantities of TNFα and IL-6, and approximately 20 % less IL-1β compared to *C. albicans*-stimulated cells. In case of Th-derived cytokines, we found that *C. parapsilosis* induced significantly lower IFNγ, and higher IL-10 secretion after 48 h compared to *C. albicans*. Furthermore, *C. parapsilosis* stimulated significantly lower IL-17 and IL-22 production after 7 days. Flow cytometric analysis following intracellular cytokine staining confirmed that there was a lower number of IL-17-producing cells in the $CD4^+$ Th population. These results suggest that while *C. albicans* induces a Th1/Th17-dominant Th polarization, *C. parapsilosis* skews the Th balance to the Th2/Treg direction.

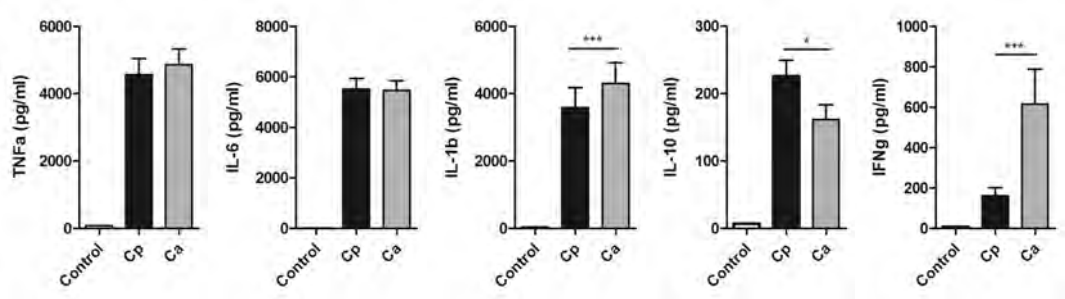

Fig. 15. Cytokine production of human PBMCs stimulated with heat-killed *C. albicans* (Ca) or *C. parapsilosis* (Cp). n=14.

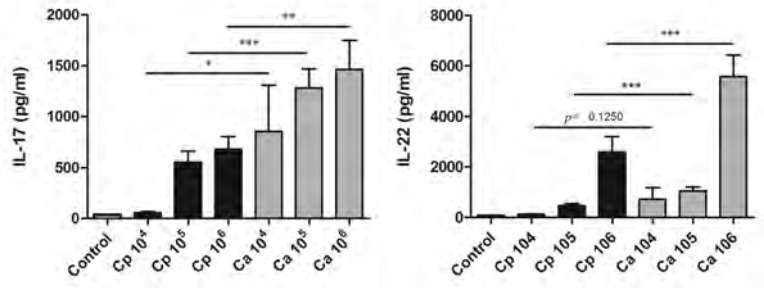

Fig. 16. IL-17 and IL-22 production by peripheral blood mononuclear cells (PBMCs) stimulated with heat-killed *C. albicans* or *C. parapsilosis*.

Identification of receptors involved in the immune recognition of C. parapsilosis

We next examined the role of Dectin-1, TLR4 and TLR2 in the cytokine production induced by *C. parapsilosis* and *C. albicans*. Following the blocking of Dectin-1, both *C. parapsilosis*- and *C. albicans*-stimulated PBMCs showed significantly lower cytokine (TNFα, IL-1β, IL-6, IL-10, IFNγ) production, indicating that the receptor plays an important role in the recognition of both species. On the other hand, while inhibition of TLR4 did not affect the cytokine production of PBMCs, our results show that TLR2 is involved in the induction of IL-1β and IL-6. However, there was no difference in the cytokine production of *C. parapsilosis*- and *C. albicans*-stimulated PBMCs during receptor blocking (although we detected a greater decrease in the levels of TNFα, IL-1β, IL-6 and IL-10 following the inhibition of Dectin-1 in *C. parapsilosis*-stimulated cells), indicating that other receptors may be responsible for the different cytokine patterns induced by the two species. Our group is currently working on the identification of other receptors that might participate in the recognition of *C. parapsilosis*.

Examination of intracellular signaling following the recognition of C. parapsilosis

The MAPK cascade plays a role in signal transduction following the activation of both TLRs and CLRs, but the role of individual MAP kinases in signaling is less clear. We found that inhibition of the three classical MAP kinases (p38, ERK, JNK) resulted in decreased TNFα, IL-1β, IL-6, IL-10, IFNγ production in both *C. parapsilosis*- and *C. albicans*-stimulated PBMCs, indicating that all three enzymes are involved in the signal transduction following the recognition of *C. parapsilosis* and *C. albicans*. Furthermore, while the inhibition of p38 and ERK resulted in a greater decrease in the levels of cytokines (TNFα, IL-1β, IL-6) in *C. parapsilosis*-stimulated cells, blocking the activity of JNK caused a more pronounced decrease in the cytokine secretion of *C. albicans*-stimulated cells. These results suggest that there is a difference in the relative contribution of p38, ERK and JNK to the resulting cytokine responses in *C. parapsilosis*- and *C. albicans*-stimulated PBMCs.

8. Comparison of inflammasome activation induced by *C. parapsilosis* and *C. albicans*

We next examined the production of cytokines in PBMCs stimulated with live *C. parapsilosis* and *C. albicans*. We found that while both species induced similar TNFα and IL-6 production, PBMCs infected with *C. parapsilosis* produced significantly less IL-1β compared to *C. albicans*-stimulated cells. Next we examined the potential mechanisms underlying this difference. The production of mature IL-1β in monocytes and macrophages is dependent on caspase-1 and the activation of the inflammasome; however, while caspase-1 is constitutively active in monocytes, in macrophages it is activated by the cleavage of pro-caspase-1 during inflammasome activation. During our study, we examined the activation of the inflammasome in PMA-treated THP-1 macrophages. We found that *C. parapsilosis* induced the secretion of IL-1β only after a relatively long incubation and when added in a high dose, while *C. albicans* induced high levels of IL-1β already after a few hours. Although, hyphae formation has been shown to play an important role in inflammasome activation by *C. albicans*, our results show

that secretion of IL-1β is independent of the presence of pseudohyphae following stimulation with *C. parapsilosis*. Furthermore, we found that the level of IL-1β mRNA and pro-IL-1β in THP-1 cells was similar following stimulation with *C. albicans* or *C. parapsilosis*, indicating that the difference in secreted IL-1β levels originates from the differential processing of IL-1β protein.

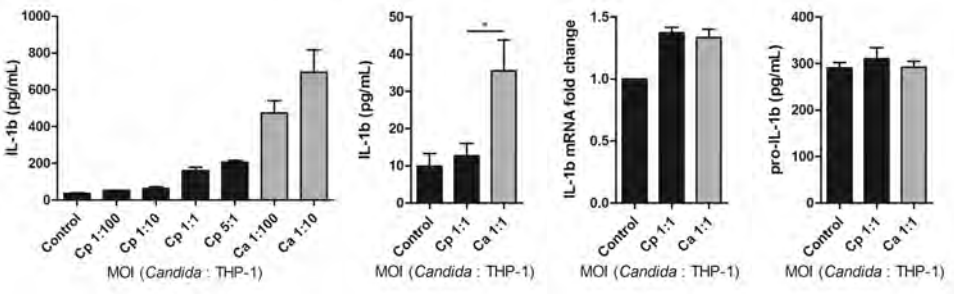

Fig. 17. Production of IL-1b by PMA-induced THP-1 monocytes in response to live *C. albicans* (Ca) and *C. parapsilosis* (Cp). From left to right: IL-1b secretion of THP-1 cells after 24 h stimulation; IL-1b production of THP-1 cells after 1 h; expression of IL-1b mRNA in THP-1 cells after 1 h; levels of pro-IL-1b in THP-1 cells after 1 h stimulation. MOI: multiplicity of infection.

Using different chemical inhibitors, we showed that mature IL-1β is produced by a similar mechanism in *C. parapsilosis*- and *C. albicans*-stimulated THP-1 cells, and the process is dependent on caspase-1, caspase-8, Syk and TLR4. Using NLRP3- and ASC-deficient THP-1 macrophages, we confirmed that IL-1β secretion in response to *C. parapsilosis* and *C. albicans* is NLRP3 inflammasome-dependent.

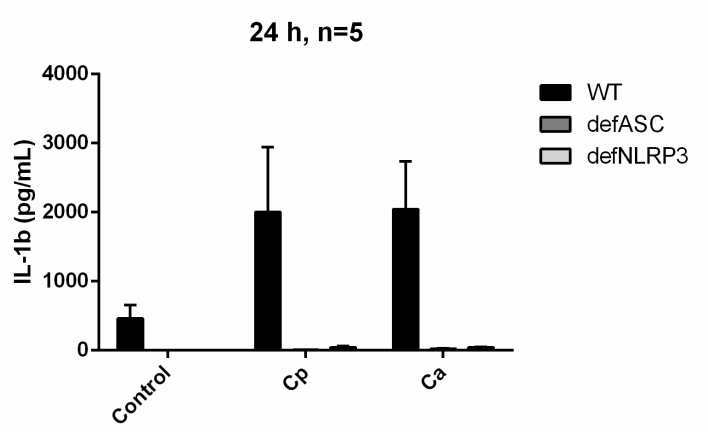

Fig. 18. IL-1b production of WT, ASC-deficient or NLRP3-deficient THP-1 macrophages following C. parapsilosis (Cp) or C. albicans (Ca) stimulation.

The three most important mechanisms involved in the activation of the NLRP3 inflammasome in macrophages is the production of ROS, release of lysosomal cathepsin B and the decrease of intracellular K^+ concentration. Our results show that IL-1β secretion following *C. parapsilosis* and *C. albicans* stimulation is K^+-efflux-dependent. However, inhibition of cathepsin B did not affect the production of IL-1β, although *C. albicans* induced higher cathepsin B release in THP-1 cells compared to *C. parapsilosis*. Furthermore, inhibition of NADPH-oxidase significantly decreased the levels of both intracellular pro-IL-1β and secreted IL-1β in THP-1 cells, indicating

the possible role of ROS in inflammasome activation. Furthermore, *C. albicans* induced significant ROS production in THP-1 cells, while *C. parapsilosis* did not induce the generation of ROS during the first four hours of infection. We also showed that the secretion of IL-1β is dependent on phagocytosis, and that *C. albicans* cells are phagocytosed more rapidly by THP-1 macrophages than *C. parapsilosis* cells. Taken together, our results suggest that multiple mechanisms play a role in the relatively low IL-1β production during *C. parapsilosis* infection. We are currently working on further details of inflammasome activation induced by *C. parapsilosis* and *C. albicans*, and we are hoping that future experiments will improve our understanding of the inflammatory response induced by the two *Candida* species.

9. Interactions between human macrophages and *Candida parapsilosis* – modulation of host immune response by secreted fungal lipases

In the present study, we compared the response of human peripheral blood monocyte-derived macrophages to a wild type (wt) as well as a lipase deficient ($lip^{-/-}$) *C. parapsilosis* strain that has been previously established in our lab. When co-cultured with macrophages, both strains induced a significant increase in the expression of tumor necrosis factor α (TNFα), interleukin-1β (IL-1β), interleukin-6 (IL-6), interleukin-8 (IL-8) and PTGS-2 (prostaglandin-endoperoxide synthase 2) genes in host cells after 12 hours, as determined by quantitative real-time PCR. Notably, macrophages stimulated with lipase mutant *C. parapsilosis* showed at least two-fold higher expression of these pro-inflammatory mediators compared to those infected with lipase-producing (wt) *C. parapsilosis.* Furthermore, the $lip^{-/-}$ *C. parapsilosis* strain induced significantly higher TNFα, IL-1β and IL-6 protein production in macrophages after 24 hours compared to the wt strain. Additionally, we examined the phagocytosis of wt and $lip^{-/-}$ *C. parapsilosis* strains by human macrophages using quantitative imaging flow cytometry. We found that although after 2 hours both strains were phagocytosed to the same extent by host cells, the rate of internalization and phagolysosome fusion was higher in case of $lip^{-/-}$ *C. parapsilosis.* These findings confirm the role of fungal lipases as important virulence factors during *C. parapsilosis* infection, and support the hypothesis that these microbial compounds have anti-inflammatory potential. Taken together, our results contribute to the better understanding of the immune response induced by *C. parapsilosis,* and highlight the role of fungal lipases during host-pathogen interactions.

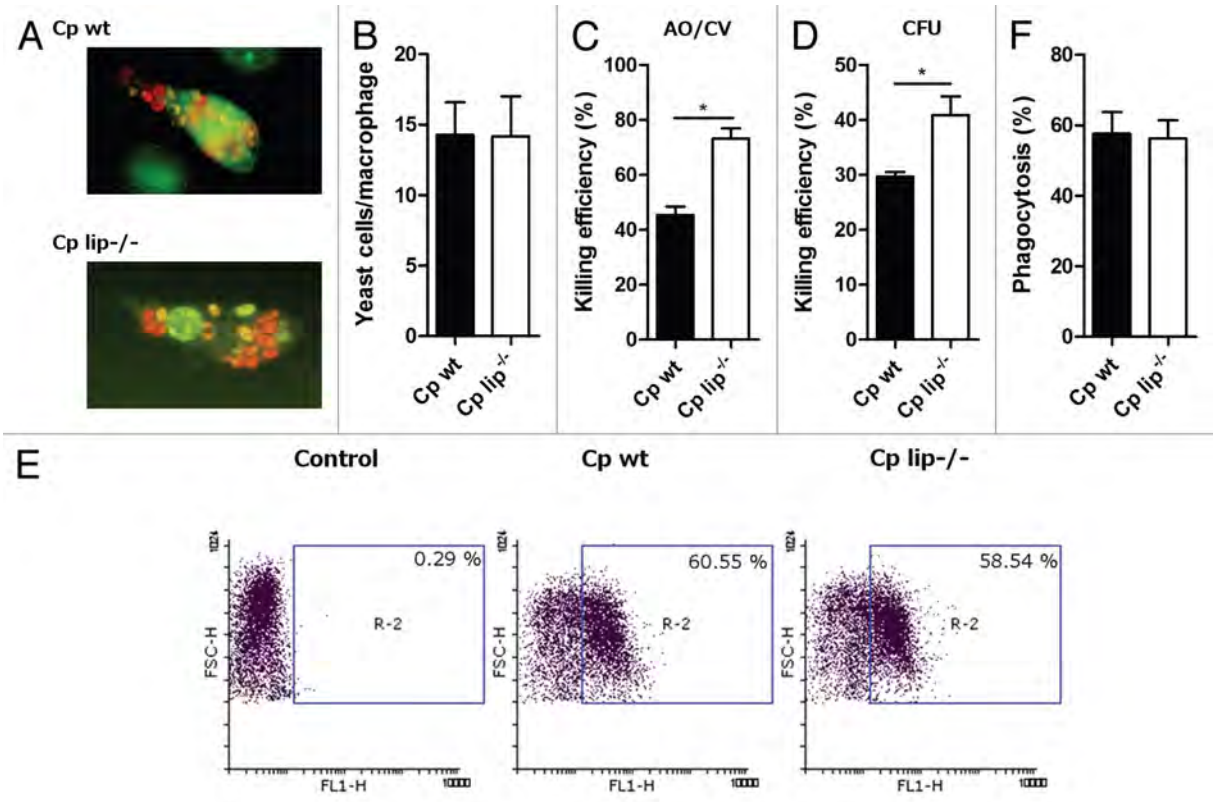

Fig. 19. Phagocytosis and killing of wt and lip−/− *C. parapsilosis* cells by human monocyte-derived macrophages. (**A**) Representative fluorescent microscopic images of human macrophages co-cultured for 3 h wt or lip−/− *C. parapsilosis*. Green fluorescence of acridin orange dye indicates live cells with intact DNA, while dead cells with degraded DNA show red fluorescence. (**B**) Phagocytosis of wt and lip−/− *C. parapsilosis* as determined by fluorescent microscopic analysis following acridin orange staining. Data are from three independent experiments and represent the average numbers of yeast cells engulfed by one macrophage (only phagocytosing macrophages were included in the analysis). (**C**) Killing of wt and lip−/− *C. parapsilosis* as determined by fluorescent microscopic analysis. Data represent the percent of dead yeast cells ± SE M. AO/CV, acridin orange/crystal violet. (**D**) Killing of wt and lip−/− *C. parapsilosis* cells by human macrophages as measured by CFU-determinations. Experiments were performed in triplicate. Data represent killing efficiency ± SE M for three donors. (**E and F**) Phagocytosis of wt and lip−/− *C. parapsilosis* cells by human macrophages analyzed by flow cytometry. Yeast cells were labeled with FITC or AlexaFluor647 and co-cultured with macrophages for 2 h. Data are from three independent experiments which were performed in duplicate. Representative dot plots (**E**) and summarized data (**F**) of the flow cytometric analysis are shown. Cp, *C. parapsilosis*; wt, wild type; lip−/−, lipase mutant; **P* < 0.05, ***P* < 0.01.

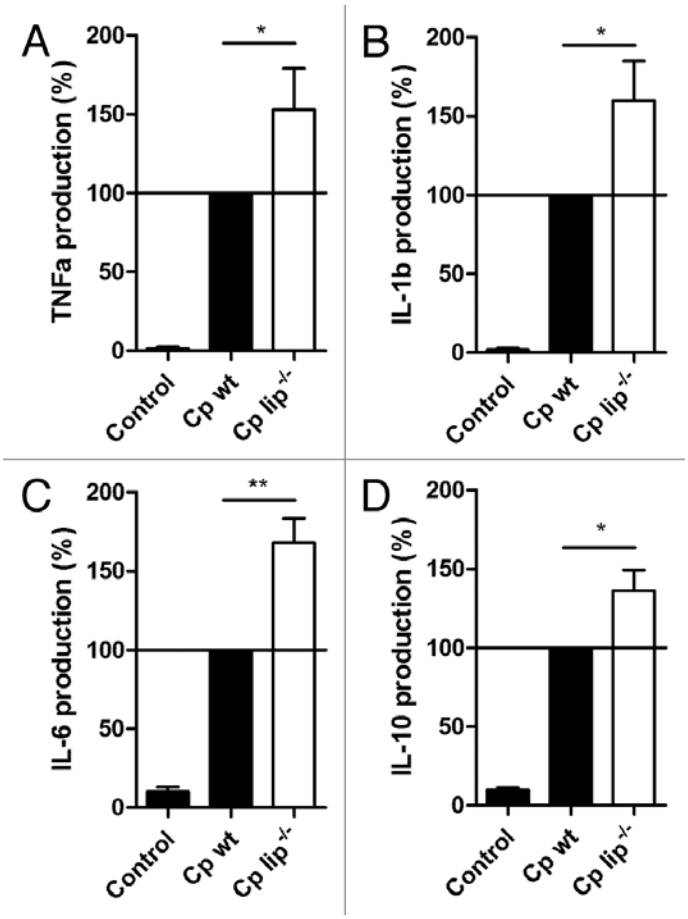

Fig. 20. Cytokine secretion of human macrophages in response to wt and lip−/− *C. parapsilosis*. Secreted TNFα (**A**), IL-1β (**B**), IL-6 (**C**), and IL-10 (**D**) levels were measured by ELISA after stimulation of macrophages with wt or lip−/− *C. parapsilosis* for 24 h. Data were normalized for each donor to cytokine levels induced by wt *C. parapsilosis* (100%) to minimize donorto- donor variability. Data represent % cytokine production ± SE M for 8 donors. Cp, *C. parapsilosis*; wt, wild type; lip−/−, lipase mutant; **P* < 0.05, ***P* < 0.01.